J Geom Anal
DOI 10.1007/s12220-014-9493-2

Numerical Solutions of Kähler–Einstein Metrics on $\mathbb{P}^2$ with Conical Singularities along a Smooth Quadric Curve

Chi Li

Received: 4 December 2013

Abstract We solve for the $SO(3)$-invariant Kähler–Einstein metric on $\mathbb{P}^2$ with cone singularities along a smooth quadric curve using a numerical approach. The numerical results show the sharp range of angles ($(\pi/2, 2\pi]$) for the solvability of equations, and the correct limit metric space ($\mathbb{P}(1, 1, 4)$). These results exactly match our theoretical conclusion. We also point out the cause of incomplete classifications in Conti (Commun Math Phys 3:751–774, 2007).

Keywords Conical Kähler–Einstein · Numerical solution · Sasaki–Einstein metrics

1 Introduction

Let D be a smooth quadric curve in $\mathbb{P}^2$. In this work, we fix $D = \{Z_1^2+Z_2^2+Z_3^2 = 0\}$. In the recent work [1], we have considered the problem of existence of Kähler–Einstein metrics on $\mathbb{P}^2$ with cone singularities along D of cone angle $2\pi\beta \in (0, 2\pi]$. The following is the main result in this study [1]:

Theorem 1.1 ([1]) *There exists a conical Kähler–Einstein metric on* $(\mathbb{P}^2, (1-\beta)D)$ *if and only if* $\beta \in (1/4, 1]$.

As pointed out to us by Dr. H-J. Hein, when $\beta = \frac{1}{3}$, this gives rise to a Calabi–Yau cone metric on the 3-dimensional A_2 singularity $x_1^2 + x_2^2 + x_3^2 + x_4^3 = 0$.

This is a question raised by Gauntlett–Martelli–Sparks–Yau in [2]. In [2], they proved that there cannot exist such Calabi–Yau cone metrics on 3-dimensional A_{k-1}

Communicated by Steven Zelditch.

C. Li (✉)
Department of Mathematics, SUNY at Stony Brook, New York, NY, USA
e-mail: chi.li@stonybrook.edu

Published online: 14 May 2014

singularities $x_1^2 + x_2^2 + x_3^2 + x_4^k = 0$ if $k \geq 4$. The idea is to look at the links L_k of such singularities. Any such Calabi–Yau cone metric would induce a Sasaki–Einstein structure on L_k. By further taking the quotient by the $U(1)$ action generated by the natural Reeb vector field, we would get an orbifold Kähler–Einstein metric on $\left(\mathbb{P}^2, \left(1-\frac{1}{k}\right) D\right)$. In [2], the obstruction for $k \geq 4$ comes from the Lichnerowicz obstruction. In [1] this was explained as $\left(\mathbb{P}^2, \left(1-\frac{1}{k}\right) D\right)$ being not log-K-polystable if $k \geq 4$. For the $k = 1$ and $k = 2$ cases, we have the standard examples corresponding to $\mathbb{P}^2$ with the Fubini–Study metric and $\left(\mathbb{P}^2, \frac{1}{2} D\right) \cong \mathbb{P}^1 \times \mathbb{P}^1$ with the product metric. This discussion leaves open the existence problem when $k = 3$.

The new insight from [1] is that we can put such kinds of orbifold Kähler metrics in the broader family of conical Kähler metrics. In our notation, $\beta = 1/k$. This allows us to apply a uniform theory which together with an interpolation argument leads us to Theorem 1.1.

However, as pointed out in [1], such a result is in contradiction to the result by Conti in [3], which says there is no cone Calabi–Yau cone metric on A_2 singularities. His proof is by classifying all the cohomogeneity one 5-dimensional Sasaki–Einstein manifolds. This leaves us wondering which one is correct.

We decide to attack this question by returning to the approach in [2] where the equations of orbifold Kähler–Einstein metrics on $(\mathbb{P}^2, (1-1/k)D)$ were written down. Note that because of $SO(3)$ symmetry, such equations come from the work in [4]. Moreover, the transformation and change of variables introduced in [2] are very useful for dealing with the problem at hand. In this way, we get a second-order differential equation with appropriate boundary conditions.

Since we could not integrate the equation for general β we will use numerical simulation to solve it. This was suggested in [2]. Our goal is to carry out such a numerical approach. As it turns out, the result is the same as we expected.

Theorem 1.2 *The equations corresponding to $SO(3)$-invariant Kähler–Einstein metric ω_β on $(\mathbb{P}^2, (1-\beta)D)$ have a numerical solution if and only if $\beta > 1/4$.*

As suggested by Dr. Song Sun and Dr. H-J. Hein, we will further verify the conjecture proposed in [1] which predicts the limit metric space as β goes to the critical value $1/4$. Again, the numerical result fits well with our expectation.

Theorem 1.3 *Numerically, as $\beta \to 1/4$, the metric space $(\mathbb{P}^2, \omega_\beta)$ converges to the metric space $(\mathbb{P}(1,1,4), \hat{\omega}_{KE})$, where $\hat{\omega}_{KE}$ is the induced orbifold Kähler–Einstein metric coming from the standard Fubini–Study metric on $\mathbb{P}^2$ by the natural branch covering: $\mathbb{P}(1,1,1) \to \mathbb{P}^2(1,1,4)$. Moreover, the bubble out of this convergence is the $\mathbb{Z}_2$-quotient of the Eguchi–Hanson metric on $\mathbb{P}^2 \backslash D$.*

The precise meaning of the above statement is detailed in Sects. 4 and 5. These results confirm our result in Theorem 1.1. In the last section, we return to calculate the data of Sasaki–Einstein 5-manifolds associated with $\mathbb{P}^1 \times \mathbb{P}^1$ and $\mathbb{P}^2$ in the sense of that in [3]. We find that there are indeed cases ignored in [3].

The example of the pair $(\mathbb{P}^2, D)$ here can be generalized in much broader settings, which we plan to discuss elsewhere together with S. Sun and H-J. Hein.

The organization of this note is as follows. The first section gives a detailed review of the structure of $SO(3)$-orbits for $\mathbb{P}^2$. The second section discusses the equations we want to solve. Again, we carefully review the approach in [2] and work out more details. In the third sections, we show our first numerical result Theorem 1.2. In Sect. 5, after describing the $SU(2)$-orbits of $\mathbb{P}(1, 1, 4)$ we demonstrate our numerical studies that explain Theorem 1.3. In the last section, we calculate the data for $\mathbb{P}^1 \times \mathbb{P}^1$ in detail. We also calculate the data for the associated Sasaki–Einstein metric which indicates the missing case in [3].

2 $SO(3)$ Orbits

Let us first review how to decompose $\mathbb{P}^2$ into $SO(3, \mathbb{R})$ orbits following [2]. First note that $\mathbb{P}^2 = (\mathbb{C}^3 - \{0\})/\mathbb{C}^*$ under the equivalence relation $(Z_1, Z_2, Z_3) \sim (\lambda Z_1, \lambda Z_2, \lambda Z_3)$ for some $\lambda \neq 0 \in \mathbb{C}^*$. Now fix any $0 \neq Z := (Z_i)_{i=1}^3 \in \mathbb{C}^3$; it determines a point in $\mathbb{P}^2$ with homogeneous coordinate $[Z] := [Z_i]_{i=1}^3 = [Z_1, Z_2, Z_3]$. Now write the polar decomposition

$$Z_1^2 + Z_2^2 + Z_3^2 = \rho^2 e^{2i\theta}.$$

So if we define

$$\tilde{Z}_i = e^{-i\theta} Z_i,$$

then $[Z_i]_{i=1}^3 = [\tilde{Z}_i]_{i=1}^3$ and

$$\tilde{Z}_1^2 + \tilde{Z}_2^2 + \tilde{Z}_3^2 = \rho^2 \geq 0. \tag{1}$$

Now write

$$\tilde{Z}_i = u_i + \sqrt{-1} v_i;$$

then the identity (1) is equivalent to the identity

$$|u|^2 - |v|^2 = \rho^2; \quad u \cdot v = 0. \tag{2}$$

We use these two relations to define the set

$$\mathbb{O} = \{(u, v) := u + iv \neq 0 | u \cdot v = 0, |u|^2 - |v|^2 \geq 0\} \subset (\mathbb{R}^3)^2 - \{0\}.$$

Define an equivalence relation on $\mathbb{O}$ by[1]

$$\begin{cases} (u, v) \sim a(u, v), & \forall a \in \mathbb{R}^\times, & \text{if } |u| \neq |v|; \\ (u, v) \sim a e^{i\theta}(u, v), & \forall a \in \mathbb{R}^\times, \forall \theta \in [0, 2\pi), & \text{if } |u| = |v|. \end{cases}$$

[1] Dr. Caner Koca pointed out to me that in the second case, the multiplication of $e^{i\theta}$ was missing in the previous version of the paper.

Denote the quotient set by $\overline{\mathbb{O}} = \mathbb{O}/\sim$. Then we have defined a homeomorphism

$$\begin{aligned} \Phi : \mathbb{P}^2 &\longrightarrow \overline{\mathbb{O}} \\ [Z_i]_{i=1}^3 &\mapsto [u, v] \text{ satisfying } u + \sqrt{-1}v = e^{-\frac{i}{2}\mathrm{Arg}(Z_1^2+Z_2^2+Z_3^2)}(Z_1, Z_2, Z_3). \end{aligned}$$

Here we assume Arg(0) can be any real number, which is compatible with the second case in the equivalence. Then $SO(3)$ acts on $\mathbb{P}^2 \cong \overline{\mathbb{O}}$ by

$$g \cdot (u, v) = (gu, gv).$$

The quotient of this action is an interval:

$$\begin{aligned} R : \overline{\mathbb{O}} &\longrightarrow [0, 1] \\ [u, v] &\mapsto \frac{|v|}{|u|}. \end{aligned}$$

So the function R classifies $SO(3)$ orbits. Moreover, it is clear that equivalently we have the identity

$$\frac{|Z_1^2 + Z_2^2 + Z_3^2|}{|Z_1|^2 + |Z_2|^2 + |Z_3|^2} = \frac{1 - R^2}{1 + R^2}. \tag{3}$$

For each point $(u, v) \in \mathbb{O}$, we get an orthonormal basis in the following way. If $v \neq 0$, we set $(e_u = u/|u|, e_v = v/|v|, e_w := e_u \times e_v)$. If $v = 0$ we choose any e_v perpendicular to $e_u = u/|u|$ and let $e_w = e_u \times u_v$. We will denote $U(1)_1$, $U(1)_2$, and $U(1)_3$ to be the rotation around the axes in the direction e_u, e_v, and e_w, respectively.

Lemma 2.1 *The generic orbit is* $\mathrm{Orb}_{R=R_0} = SO(3)/\mathbb{Z}_2$ *(when* $0 < R_0 = R([u, v]) < 1$*). The two special orbits are*

$$\begin{aligned} \mathrm{Orb}_{R=0} &= (SO(3)/\mathbb{Z}_2)/U(1)_1 = \mathbb{RP}^2; \\ \mathrm{Orb}_{R=1} &= (SO(3)/\mathbb{Z}_2)/U(1)_3 = \mathbb{P}^1. \end{aligned}$$

Proof When $0 < R = \frac{|v|}{|u|} < 1$, the stabilizer of $SO(3)$ action at $[v, w]$ is isomorphic to $\mathbb{Z}_2$ with the generator being the rotation around e_w with angle π, i.e., $(e_u, e_v, e_w) \to (-e_u, -e_v, e_w)$.

When $R = 0$, v=0. The stabilizer is generated by $\mathbb{Z}_2$ and $U(1)_1$. The generator of $\mathbb{Z}_2$ can be chosen to be $(e_u, e_v, e_w) \mapsto (-e_u, -e_v, e_w)$ (for any e_v, e_w such that $\{e_u, e_v, e_w\}$ is an orthonormal basis). $U(1)_1$ is the rotation group around e_u. It is easy to verify that

$$\mathrm{Orb}_{R=0} = (\mathbb{R}^3 - \{0\})/\mathbb{R}^\times = \mathbb{RP}^2.$$

When $R = 1$, $|u| = |v|$. The stabilizer is the $U(1)$-rotation group around e_w denoted as $U(1)_3$. Note $\mathbb{Z}_2 \subset U(1)_3$. It is easy to see that (for example, by (3))

$$\mathrm{Orb}_{R=1} = \{Z_1^2 + Z_2^2 + Z_3^2 = 0\} \cong \mathbb{P}^1 \subset \mathbb{P}^2.$$

□

Fix the generator of $so(3) = \mathrm{Lie}(SO(3))$ to be

$$X_1 = \begin{pmatrix} 0 & 0 & 0 \\ 0 & 0 & -1 \\ 0 & 1 & 0 \end{pmatrix}, \quad X_2 = \begin{pmatrix} 0 & 0 & 1 \\ 0 & 0 & 0 \\ -1 & 0 & 0 \end{pmatrix}, \quad X_3 = \begin{pmatrix} 0 & -1 & 0 \\ 1 & 0 & 0 \\ 0 & 0 & 0 \end{pmatrix}.$$

Then the corresponding invariant vector field on the orbit $SO(3)([u, v])$ at a point $[u, v]$ is given by the infinitesimal rotation around three axes in the directions of e_u, e_v, e_w, respectively. In other words, they are generators of the actions of $U(1)_1, U(1)_2, U(1)_3$, respectively.

1. Around e_u:

$$T_u = \left.\frac{d}{d\theta}\right|_{\theta=0} (u + \sqrt{-1}(\cos\theta e_v - \sin\theta e_w)|v|) = -\sqrt{-1}|v|e_w.$$

2. Around e_v: $T_v = \left.\frac{d}{d\theta}\right|_{\theta=0} (\sin\theta e_w + \cos\theta e_u)|u| + \sqrt{-1}v = |u|e_w.$
3. Around e_w:

$$\begin{aligned} T_w &= \left.\frac{d}{d\theta}\right|_{\theta=0} (|u|(\cos\theta e_u - \sin\theta e_v) + \sqrt{-1}(\sin\theta e_u + \cos\theta e_v)|v|) \\ &= -|u|e_v + \sqrt{-1}|v|e_u. \end{aligned}$$

We can define another vector field generating the radial transformation

$$T_R = \left.\frac{d}{d\theta}\right|_{\theta=0} \left(|u|(e_u + \sqrt{-1}\left(\frac{|v|}{|u|} + \theta\right) e_v\right) = \sqrt{-1}|u|e_v.$$

Note that the above vectors represent the tangent vector in

$$T_{[u+iv]}\mathbb{P}^2 = \mathrm{Hom}(\mathbb{C}(u + iv), (\mathbb{C}(u + iv))^{\perp}) \cong \mathrm{Hom}(\mathbb{C}(u + iv), \mathbb{C}^3/\mathbb{C}(u + iv)).$$

Lemma 2.2 *On* $\mathrm{Orb}_{R=0} = \mathbb{RP}^2$, $T_u = 0$*; on* $\mathrm{Orb}_{R=1} = \mathbb{P}^1$, $T_w = 0$.

Proof When $R = 0$, $|v| = 0$, so $T_u = 0$ on $\mathrm{Orb}_{R=0}RP^2$. When $R = 1$,

$$T_w = |u|\frac{v}{|v|} - \sqrt{-1}|v|\frac{u}{|u|} = -\sqrt{-1}(u + \sqrt{-1}v)$$

so $T_w = -\sqrt{-1}(u + \sqrt{-1}v) \in \mathbb{C} \cdot (u, v)$, so $T_w|_{R=1} = 0$, i.e., T_w vanishes on the special orbits $\mathrm{Orb}_{R=1} = \mathbb{P}^1$. □

Note that this lemma also follows from Lemma 2.1 by the fact that $U(1)_1$ is the stabilizer group on $\mathrm{Orb}_{R=0}$ generated by T_u, while $U(1)_3$ is the stabilizer group on $\mathrm{Orb}_{R=1}$ generated by T_w.

3 Equations for $SO(3)$ Invariant Kähler–Einstein

For special metrics g on $\mathbb{P}^2$, we have the following

Lemma 3.1 *1. For any Kähler metric g, we have $|T_u|_g \le |T_v|_g$. The equality holds only on the special orbit* $\mathrm{Orb}_{R=1} = \mathbb{P}^1$.
2. *For any $SO(3)$ invariant metric g, $|T_v|_g = |T_w|_g$ on the special orbit* $\mathrm{Orb}_{R=0} = \mathbb{RP}^2$.

Proof 1. A Kähler metric is compatible with the complex structure $J = i\cdot$, so

$$0 \le \frac{|T_u|_g}{|T_v|_g} = \frac{|i|v|e_w|_g}{||u|e_w|_g} = \frac{||v|e_w|_g}{||u|e_w|_g} = \frac{|v|}{|u|} = R \le 1. \tag{4}$$

2. On the special orbit $\mathrm{Orb}_{R=0} = \mathbb{RP}^2$, $v = 0$. Let $\gamma_1(\theta) = |u|(\sin\theta e_w + \cos\theta e_u)$ and $\gamma_2(\theta) = |u|(\cos\theta e_u - \sin\theta e_v)$. Then $T_v = \gamma_1'(0)$ and $T_w = \gamma_2'(0)$. Because there exist rotations $g(\theta)$ in $SO(3)$ such that $g(\theta)\cdot\gamma_1(\theta) = \gamma_2(\theta)$, the conclusion follows from invariance of the metric under $SO(3)$.

□

Now choose the dual basis of $\{T_R, T_u, T_v, T_w\}$ to be one form given by $\{dR, \sigma_1, \sigma_2, \sigma_3\}$. For any $SO(3)$ invariant Kähler metric on $\mathbb{P}^2$, $\{T_u, T_v, T_w, T_R\}$ is orthogonal. The metric can be written in the form

$$g = (dt)^2 + a^2\sigma_1^2 + b^2\sigma_2^2 + c^2\sigma_3^2, \tag{5}$$

where

$$dt = -|T_R|_g dR, \quad a = |T_u|_g, \quad b = |T_v|_g, \quad c = |T_w|_g.$$

The minus sign in the first identity is to make the special orbit $\mathbb{P}^1$ sit in the distance 0 location. By Lemma 2.2 and 3.1, we know that

Corollary 3.1 *For any $SO(3)$-invariant Kähler metric on $\mathbb{P}^2$, we have $a \le b$ on $\mathbb{P}^2$. On* $\mathrm{Orb}_{R=1} = \mathbb{P}^1$, $c = 0$, $a = b$. *On* $\mathrm{Orb}_{R=0} = \mathbb{RP}^2$, $a = 0$, $b = c$.

Example 3.1 When $\beta = 1$, the $SO(3)$ invariant metric is the standard Fubini–Study metric on $\mathbb{P}^2$. We can write it in the form of (5). One way to do this is to recall the following description of the Fubini–Study metric. Let $\gamma(t) := [Z_1(t), Z_2(t), Z_3(t)]$ be a curve in $\mathbb{P}^2$ with the tangent vector $\gamma'(0) = ((Z_1(0), Z_2(0), Z_3(0)) \mapsto (Z_1'(0), Z_2'(0), Z_3'(0))) \in \mathrm{Hom}(\mathcal{O}_{\mathbb{P}^2}(1), \mathbb{C}^3/\mathcal{O}_{\mathbb{P}^2}(1))$. The length of $\gamma'(0)$ is given by

$$|\gamma'(0)|^2_{FS} = \frac{|Z'(0)^{\perp}|^2}{|Z(0)|^2} = \left(|Z'(0)|^2 - \frac{|\langle Z'(0), Z(0)\rangle|^2}{|Z(0)^2|}\right)/|Z(0)|^2,$$

where $\langle \cdot, \cdot \rangle$ is the standard Hermitian inner product on $\mathbb{C}^3 \cong \mathbb{R}^6$. Using this formula, it is easy to verify that

$$|T_R|_{FS} = \frac{|u|^2}{|u|^2+|v|^2} = \frac{1}{1+R^2}, \qquad |T_u|_{FS} = \frac{|v|}{\sqrt{|u|^2+|v|^2}} = \frac{R}{\sqrt{1+R^2}}$$

$$|T_v|_{FS} = \frac{|u|^2}{\sqrt{|u|^2+|v|^2}} = \frac{1}{\sqrt{1+R^2}}, \qquad |T_w|_{FS} = \frac{|u|^2-|v|^2}{|u|^2+|v|^2} = \frac{1-R^2}{1+R^2}.$$

So the normal distance function t is determined by

$$dt = -\frac{1}{1+R^2} dR \quad and \quad t(1) = 0 \Longrightarrow R = \tan\left(\frac{\pi}{4} - t\right).$$

So $0 \le t \le \pi/4$ and

$$a = \sin\left(\frac{\pi}{4} - t\right) = \cos\left(t + \frac{\pi}{4}\right), \quad b = \sin\left(t + \frac{\pi}{4}\right), \quad c = \cos\left(\frac{\pi}{2} - 2t\right) = \sin(2t).$$

Example 3.2 The data for $\mathbb{P}^1 \times \mathbb{P}^1 = \left(P^2, \frac{1}{2}D\right)$ are given as follows. See Sect. 6 for the derivation of these data. (See also [4] and [2].)

$$a(t) = \frac{1}{\sqrt{3}}\cos(\sqrt{3}t), \quad b(t) = \frac{1}{\sqrt{3}}, \quad c(t) = \frac{1}{\sqrt{3}}\sin(\sqrt{3}t).$$

The range for t is $0 \le t \le \pi/(2\sqrt{3})$.

By [4] and [2], the equation for Kähler–Einstein with Ricci curvature equal to 3 is reduced to a system of ODEs:

$$\begin{cases} \dot{a} = -\frac{b^2+c^2-a^2}{2bc} \\ \dot{b} = -\frac{a^2+c^2-b^2}{2ac} \qquad 0 \le t \le t_* = t_{max} \\ \dot{c} = -\frac{a^2+b^2-c^2}{2ab} + 6ab. \end{cases} \tag{6}$$

Note that the equation in [2] differs from [4] by a (negative) factor $(-abc)$ which is caused by a change of variable.

The boundary condition at $t = 0$ corresponds to the special orbit $\mathrm{Orb}_{R=1} = \mathbb{P}^1$, where by Corollary 3.1 $a = |T_u|_g = |T_v|_g = b$ and $c = |T_w|_g = 0$. Moreover, the cone angle equal to $2\pi\beta$ along $\mathrm{Orb}_{t=0} = \mathbb{P}^1$ requires $\dot{c} = 2\beta$. The factor 2 comes from the fact that when $0 < R < 1$ the stabilizer is $\mathbb{Z}_2$. So the boundary condition is

$$a(t) = \alpha + O(t)$$
$$b(t) = \alpha + O(t)$$
$$c(t) = 2\beta t + O(t^2).$$

Note that the normalized Kähler–Einstein metric ω'_β satisfies

$$Ric(\omega'_\beta) = 3\omega'_\beta + 2\pi(1-\beta)\{D\}.$$

Because $[D] = \frac{2}{3}c_1(\mathbb{P}^2)$, by taking cohomological classes on both sides, we get

$$3[\omega'_\beta] = \frac{1}{3}(1+2\beta)\cdot 2\pi c_1(\mathbb{P}^2).$$

So α and β are related by $\alpha^2 = \delta\cdot\frac{1}{3}(1+2\beta)$ since both sides are proportional to the volume of $\mathbb{P}^1$. The factor δ can be carefully tracked out, but it can also be easily determined either by checking the standard $\mathbb{P}^2$ with the Fubini–Study metric in Example 3.1 or by substituting into the last equation in (6). The result is

$$\alpha^2 = \frac{1}{6}(1+2\beta),$$

obtained from Eq. (6).

When $t = t_* = t_{max}$, we know from Corollary 3.1 that $a(t_*) = 0$ and $b(t_*) = c(t_*)$.

Lemma 3.2

$$\dot{a}(t_*) = -1, \quad \dot{b}(t_*) = \dot{c}(t_*) = 0. \tag{7}$$

Proof From the first equation in (6) and $b(t_*) = c(t_*)$, we get $\dot{a}(t_*) = -1$. Then we use this to derive from Eq. (6) that

$$\dot{b}(t_*) = -\dot{c}(t_*) = \lim_{t\to t_*}\frac{b-c}{a} = -(\dot{b}(t_*) - \dot{c}(t_*)) = -2\dot{b}(t_*).$$

So the second identity follows. □

Note that $\dot{a}(t_*) = -1$ is compatible with the fact that the conical metric is smooth along $\mathrm{Orb}_{R=0} \cong \mathbb{RP}^2$.

Note the solution of Eq. (6) is not unique around the point $(a(0), b(0), c(0)) = (\alpha, \alpha, 0)$. There are at least three possibilities: $a \le b$, $a = b$, $a \ge b$. The $a = b$ case corresponds to the Gibbons–Pope–Pederson metric as pointed out in [4]. We are in the $a \le b$ case. The symmetry of a, b is broken by writing down the differential equation for the variable $R = a/b$. Using (6), we get

$$c\frac{d}{dt}\left(\frac{a}{b}\right) = \left(\frac{a}{b}\right)^2 - 1.$$

So it is natural to do the following change of variables introduced by [2].

$$\frac{dr}{dt} = 1/c. \tag{8}$$

Then

$$\frac{dR}{dr} = R^2 - 1.$$

Using $a \le b$ ((4)), we get the solution

$$R = \frac{a}{b} = -\tanh(r). \tag{9}$$

Moreover, we get the range for $r : -\infty < r \le 0$. We list the ranges of R, t, r as follows:

	$\mathbb{P}^2$	$SO(3)/\mathbb{Z}_2$	RP^2
R	$R = 1$	$1 > R > 0$	$R = 0$
t	$t = 0$	$0 < t < t_*$	$t = t_*$
r	$r = -\infty$	$-\infty < r < 0$	$r = 0$

Define $f = ab$. Then f satisfies the following second-order differential equation (see [2]):

$$\frac{d}{dr}\log\left(f\frac{df}{dr}\right) = 2[6f + \coth(2r)].$$

Example 3.3 By easy calculations, one can get that, for $\mathbb{P}^2$, $f = -\frac{1}{2}\tanh(2r)$, $f_r(0) = -1$; and for $\mathbb{P}^1 \times \mathbb{P}^1$, $f = -\frac{1}{3}\tanh(r)$, $f_r(0) = -\frac{1}{3}$. See [2] and also Sect. 6.

Let $h = f_r$. Then this is equivalent to a system:

$$\begin{cases} f_r &= h \\ h_r &= 12fh + 2\coth(2r)h - \frac{h^2}{f}. \end{cases} \tag{10}$$

It is easy to verify that the data (f, R, h) and (a, b, c) determine each other by the relation

$$f = ab, \quad R = \frac{a}{b}, \quad h = f_r = -c^2. \tag{11}$$

The boundary condition is given by

$$f(-\infty) = \alpha^2, f(0) = 0,$$
$$h(0) = f_r(0) = -c(t_*)^2 = -b(t_*)^2.$$

Using (7), (6) and $t_r(t) = c(t)$, we get

$$h_r(0) = f_{rr}(0) = ((f_{tt}t_r + f_t(t_r)_t)t_r)\,|_{t=t_*} = \ddot{a}(t_*)b(t_*)^3 = 0.$$

4 Numerical Studies: $\beta > 1/4$

Now we explain our numerical simulation. We introduce the variable τ for convenience and write the boundary values as $(f(0), h(0)) = \left(0, -\frac{1}{\tau} := -b(t_*)^2\right)$ and solve the Eq. (10) numerically. However, this cannot be done because there is a zero in the denominator for $r = 0$ in the second equation in (10) (although it is cancelled by zero on the numerator). We can, however, move away from $r = 0$ a little bit by using the boundary condition and Taylor expansion:

$$f(r) = f(0) + f_r(0)r + O(r^2) = -\frac{1}{\tau}r + O(r^2)$$
$$h(r) = h(0) + h_r(0)r + O(r^2) = -\frac{1}{\tau} + O(r^2).$$

So numerically, we can choose $r_0 < 0$ to be very close to 0 and choose the boundary condition to be

$$(f(r_0), h(r_0)) = \left(-\frac{r_0}{\tau}, -\frac{1}{\tau}\right).$$

For example, in the following numerical simulation, we choose $r_0 = -10^{-5}$. Then we can shoot the trajectory out for r going from r_0 backward to $-\infty$. (We will use the **NDSolve** tool in **Mathematica** in the numerical study. The code generating the figures can be found in the appendix.)

If we choose different τ, then we get different solutions of f, $h = f_r$. Figure 1 shows the numerical solutions for $\tau = 2^i$, $i = 3, \ldots, 15$. We can observe that for fixed τ, the graph will become flat as r goes toward $-\infty$, which means $f(r)$ becomes stabilized. The speed of approaching flatness depends on the boundary value $h(0) = -\frac{1}{\tau}$. The bigger τ is, the longer r-distance it takes for the graph to become flat. (This is related to the bubbling phenomenon below.)

We also observe from Fig. 1 that the value $f(-\infty)$ seems to approach $1/4 = 0.25$ as τ becomes bigger. To see this more clearly, note that $\lim_{r\to-\infty} f(r) = f(-\infty) = \alpha^2 = \frac{1+2\beta}{6}$. Numerically, we can just evaluate $f(r)$ for r being sufficiently negative

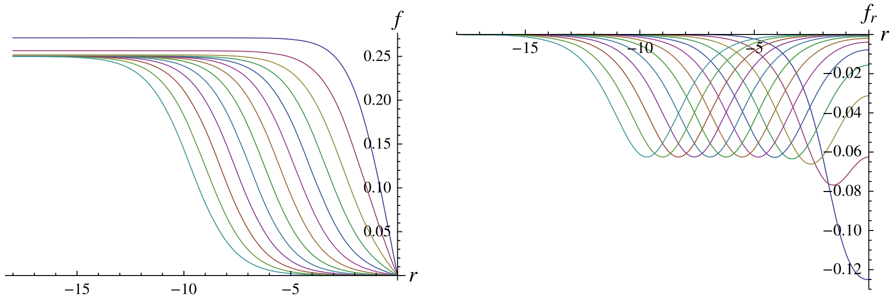

(a) (r, f) **(b)** (r, f_r)

Fig. 1 $\tau = 2^i, i = 3, \ldots, 15$

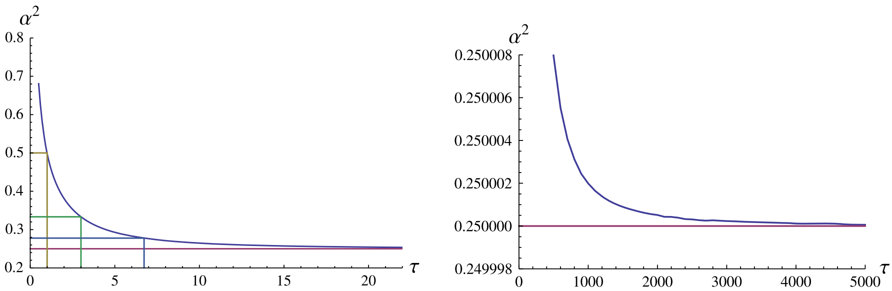

(a) short range **(b)** long range

Fig. 2 (τ, α^2)

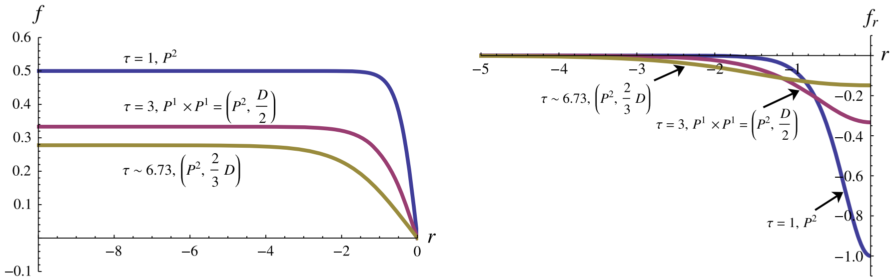

(a) (r, f) **(b)** (r, f_r)

Fig. 3 Data for $\tau = 1, 3, 6.73$

to calculate α^2. So we use **Mathematica** to calculate (very dense) sequences of data for $\{\tau,\ f(\tau, r)\}$, where we make solution f depend on the boundary data τ. Then we sample the value of $f(\tau, r)$ at $r = -500$. (One can certainly choose r to be more negative, but the visual effect does not change). Figure 2 shows the numerical result. The two subfigures are for short range and long range of τ, respectively.

We see immediately that α^2 is a decreasing function of τ. More importantly, from the picture, we see that one always has

$$\alpha^2 = \frac{1 + 2\beta}{6} > 0.25 \Longleftrightarrow \beta > \frac{1}{4},$$

and all the $\beta > \frac{1}{4}$ can be achieved. In particular, when $\beta = \frac{1}{3}$, where $\alpha^2 = \frac{5}{18} = 0.277777_{\ldots}$, one can find the approximate value of $\tau \sim 6.73$ from the numerical result. In the picture, we have identified three special points: $(1, 0.5)$, $(3, 1/3)$, and $\left(6.73,\ \frac{5}{18}\right)$, which correspond to $\beta = 1$, $\frac{1}{2}$, and $\frac{1}{3}$, respectively. Note that we are only interested when $\beta \leq 1$, or equivalently when $\alpha^2 \leq 0.5$. However, the picture suggests we can even pass $\beta \leq 1$ and solve for the conical Kähler–Einstein metric with cone angle $2\pi\beta > 2\pi$ along the smooth quadric curve.

In Fig. 3, we draw numerical solutions corresponding to $\mathbb{P}^2$ when $\tau = 1$, $\mathbb{P}^1 \times \mathbb{P}^1 = \left(\mathbb{P}^2, \frac{1}{2}D\right)$ when $\tau = 3$, and $\left(\mathbb{P}^2, \frac{2}{3}D\right)$ when $\tau \sim 6.73$. Of course, when $\tau = 1$ and

$\tau = 3$, the graphs of $f = f(r)$ just recover the graph $f(r) = -\frac{1}{2}\tanh(2r)$ for $\mathbb{P}^2$ and $f(r) = -\frac{1}{3}\tanh(r)$ for $\mathbb{P}^1 \times \mathbb{P}^1$ (up to high precision).

5 Limit as β Goes To 1/4

5.1 Metric Limit

First note that we have the following embedding:

$$\begin{aligned} \Delta : \mathbb{P}^1 &\longrightarrow \mathbb{P}^2 \\ [U_0, U_1] &\mapsto [U_0^2 + U_1^2, 2iU_0U_1, i(U_0^2 - U_1^2)]. \end{aligned}$$

$SU(2) < SL(2, \mathbb{C})$ acts on $\mathbb{P}^1$ naturally, while $SO(3, \mathbb{R}) < SO(3, \mathbb{C})$ acts on $\mathbb{P}^2$.

It is straightforward to verify that the above embedding induces a morphism between groups:

$$\varphi : SL(2, \mathbb{C}) \longrightarrow SO(3, \mathbb{C})$$
$$\begin{pmatrix} a & b \\ c & d \end{pmatrix} \mapsto \frac{1}{ad - bc} \begin{pmatrix} (a^2 + b^2 + c^2 + d^2)/2 & -i(ab + cd) & -i(a^2 - b^2 + c^2 - d^2)/2 \\ i(ac + bd) & ad + bc & ac - bd \\ i(a^2 + b^2 - c^2 - d^2)/2 & ab - cd & (a^2 - b^2 - c^2 + d^2)/2 \end{pmatrix}.$$

Note that $\phi(SU(2)) = SO(3, \mathbb{R})$ is the 2-fold covering. So the embedding Δ is equivariant with respect to the covering homomorphism $\phi : SU(2) \to SO(3, \mathbb{R})$.

Now $SU(2)$ acts on $\mathbb{P}^2(1, 1, 4)$ by acting on the first two variables:

$$g \cdot [U_0, U_1, V] = [g \cdot (U_0, U_1), V].$$

There is a natural embedding $\mathbb{P}^1 \subset \mathbb{P}(1, 1, 4)$ by the vanishing of the last coordinate. We identify this $\mathbb{P}^1$ with the image under Δ:

$$\Delta(\mathbb{P}^1) = \{Z_1^2 + Z_2^2 + Z_3^2 = 0\}.$$

Fix generators of $SU(2, \mathbb{C})$ to be standard Pauli matrices:

$$Y_1 = \begin{pmatrix} 0 & 1 \\ -1 & 0 \end{pmatrix}, \quad Y_2 = \begin{pmatrix} 0 & i \\ i & 0 \end{pmatrix}, \quad Y_3 = \begin{pmatrix} i & 0 \\ 0 & -i \end{pmatrix}.$$

Note that the commutator relation $[Y_1, Y_2] = 2Y_3$ and cyclically. So by letting $\tilde{Y}_i = \frac{Y_i}{2}$, $\tilde{Y}_i$'s satisfy $[\tilde{Y}_1, \tilde{Y}_2] = \tilde{Y}_3$ and cyclically. For simplicity, we will still use $\tilde{Y}_i$ to denote the vector fields on $\mathbb{P}(1, 1, 4)$ corresponding to the infinitesimal actions of $\tilde{Y}_i$. Then we have

Lemma 5.1 *When we restrict to* $\mathbb{P}^1$, $\Delta_* \tilde{Y}_1 = -T_u$, $\Delta_* \tilde{Y}_2 = T_v$, $\Delta_* \tilde{Y}_3 = T_w$.

Proof $\Delta(1,0) = (1,0,i) = u + iv$ with $u = (1,0,0)$ and $v = (0,0,1)$. So $w = u \times v = -(0,1,0)$.

$$\Delta_* \tilde{Y}_i = (2(U_0\dot{U}_0 + U_1\dot{U}_1), 2i(\dot{U}_0 U_1 + U_0\dot{U}_1), 2i(U_0\dot{U}_0 - U_1\dot{U}_1)).$$

1. $\tilde{Y}_1 = \frac{1}{2}(U_1, -U_0)$, so

$$\Delta_* \tilde{Y}_1 = (0, -i(U_0^2 - U_1^2), 2iU_0U_1).$$

   In particular, $\tilde{Y}_1|_{(1,0)} = \frac{1}{2}(0,-1)$ and $\Delta_*\tilde{Y}_1|_{(1,0)} = (0,-i,0) = ie_w$. So $\Delta_*\tilde{Y}_1 = -T_u$.
2. $\tilde{Y}_2 = \frac{1}{2}(iU_1, iU_0)$, so

$$\Delta_* \tilde{Y}_2 = (2iU_0U_1, -(U_0^2 + U_1^2), 0).$$

   In particular, $\tilde{Y}_2|_{(1,0)} = \frac{1}{2}(i,0)$, $\Delta_*\tilde{Y}_2|_{(1,0,i)} = (0,-1,0) = e_w$. So $\Delta_*\tilde{Y}_2 = T_v$.
3. $\tilde{Y}_3 = \frac{1}{2}(iU_0, -iU_1)$, so

$$\Delta_* \tilde{Y}_1 = (i(U_0^2 - U_1^2), 0, -(U_0^2 + U_1^2)).$$

   In particular, $\tilde{Y}_3|_{(1,0)} = \frac{i}{2}(1,0)$ and $\Delta_*\tilde{Y}_3|_{(1,0,i)} = (i,0,-1) = -v + iu$. So $\Delta_*\tilde{Y}_3 = T_w$. □

We can define a function which classifies the $SU(2)$ orbits

$$\begin{aligned} \tilde{R} : \mathbb{P}(1,1,4) &\longrightarrow [0,+\infty) \\ [U_0, U_1, V] &\mapsto \left(\frac{|U_0|^2 + |U_1|^2}{|V|^{1/2}}\right)^{1/2}. \end{aligned}$$

Lemma 5.2 *The generic orbit when* $0 < \tilde{R} < \infty$ *is isomorphic to* $SU(2)/\mathbb{Z}_4 \cong SO(3)/\mathbb{Z}_2$. *The special orbits are*

$$\mathrm{Orb}_{\tilde{R}=0} = \mathrm{Pt} = [0,0,1], \quad \mathrm{Orb}_{\tilde{R}=\infty} = \mathbb{P}^1.$$

Proof If $0 < \tilde{R} < +\infty$, then $[U_0, U_1, V]$ is the same as $[\sqrt{-1}^j U_0, \sqrt{-1}^j U_1, V]$, $j = 1,2,3,4$. So the stabilizer is isomorphic to $\mathbb{Z}_4$. The cases of special orbits are clear. □

Now the $SU(2)$-invariant Kähler metric has the form

$$g = dt^2 + a^2\sigma_1^2 + b^2\sigma_2^2 + c^2\sigma_3^2.$$

Similarly as in Example 3.1 in Sect. 2, we can calculate the induced orbifold Kähler–Einstein metric by the branch covering map:

$$\begin{aligned} \mathbb{P}(1,1,1) &\longrightarrow \mathbb{P}(1,1,4) \\ [Z_1, Z_2, Z_3] &\mapsto [Z_1, Z_2, Z_3^4]. \end{aligned}$$

Because the metric is $SU(2)$ invariant, to write down the metric we only need to calculate the length of the basic vector fields at the special point $(\tilde{R}, 0, 1)$ in each $SU(2)$-orbit.

1. $T_{\tilde{R}}|_{(\tilde{R},0,1)} = (1, 0, 0)$, $|T_{\tilde{R}}| = \frac{1}{1+\tilde{R}^2}$.
2. $\tilde{Y}_1|_{(\tilde{R},0,1)} = \frac{1}{2}(0, -\tilde{R}, 0)$, $a = |\tilde{Y}_1|_g = \frac{1}{2}\frac{\tilde{R}}{\sqrt{1+\tilde{R}^2}}$.
3. $\tilde{Y}_2|_{(\tilde{R},0,1)} = \frac{1}{2}(0, i\tilde{R}, 0)$, $b = |\tilde{Y}_2|_g = \frac{1}{2}\frac{\tilde{R}}{\sqrt{1+\tilde{R}^2}}$.
4. $\tilde{Y}_3|_{(\tilde{R},0,1)} = \frac{1}{2}(i\tilde{R}, 0, 0)$, $c = |\tilde{Y}_3|_g = \frac{1}{2}\frac{\tilde{R}}{1+\tilde{R}^2}$.

Again, we can transform to the distance function:

$$dt = -\frac{d\tilde{R}}{1+\tilde{R}^2} \text{ and } \tilde{R}(+\infty) = 0 \Longrightarrow \tilde{R} = \tan(\pi/2 - t), 0 \le t \le \pi/2.$$

By substituting $\tilde{R}$ into the expression of a, b, and c, we get the data for $\mathbb{P}(1, 1, 4)$:

$$a = b = \frac{1}{2}\sin\left(\frac{\pi}{2} - t\right) = \frac{1}{2}\cos(t)$$
$$c = \frac{1}{4}\sin(\pi - 2t) = \frac{1}{4}\sin(2t).$$

Note that in this case, $a/b \equiv 1$. This is very different from the case where $\beta > 1/4$. For the latter, $a < b$ except on the special fiber $\mathrm{Orb}_{R=1} \cong \mathbb{P}^1$, where $a = b$. Moreover, the boundary condition now becomes

$$a(t) = b(t) = 1/2 + O(t^2)$$
$$c(t) = \frac{1}{2}t + O(t^3).$$

On the other end where $t_* = \pi/2$, $a(\pi/2) = b(\pi/2) = c(\pi/2) = 0$. Geometrically, the special fiber $\mathrm{Orb}_{R=0} \cong \mathbb{RP}^2$ shrinks to a point as $\beta \to 1/4$. If we do the same transformation that $dr/dt = 1/c$, the range of r becomes $(-\infty, +\infty)$ instead of $(-\infty, 0)$ because $c(t_*) = 0$.

Next we give the numerical results which show that the metric ω_β converges to the orbifold Kähler–Einstein metric on $\mathbb{P}(1, 1, 4)$.

First we integrate the identity $dr/dt = 1/c$ numerically and plot the relation between the boundary value $b(t_*)^2 = 1/\tau$ and $t_{\max} = t_*$ (Fig. 4). We see that the maximal value for t is an increasing function of τ. As $\tau \to +\infty$, or equivalently as $\beta \to 1/4$, $t_{max} = t_*$ converges to $\pi/2$.

Note that the coordinate t is the distance function from the special orbit $\mathbb{P}^1$. So t is a geometrically meaningful coordinate in contrast with r which is only an auxiliary coordinate. So we can get a good convergence when we look the data as functions of t.

Now we can plot the graph of the data set $(f = ab, R = a/b, -f_r = c^2)$ as the function of t instead of r. (See (11)). Figure 5 shows the data for $\tau = 1.1^i$,

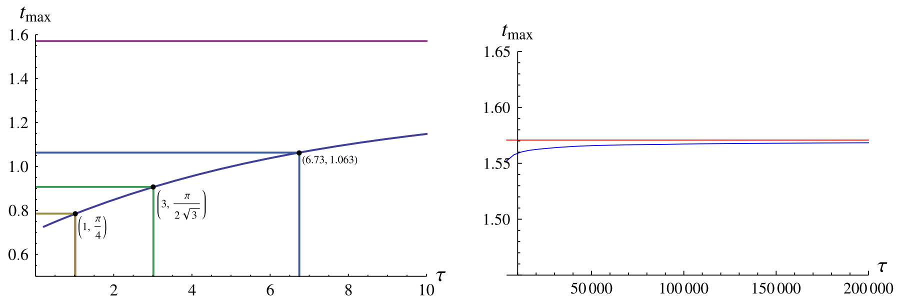

(a) short range **(b)** long range

Fig. 4 Diameter

$i = 0, 2, 4, \ldots, 120$. The thickened red curves represent the data for $\mathbb{P}(1, 1, 4)$, where

$$f(t) = a(t)b(t) = \frac{1}{4}\cos^2(t), \quad R = \frac{a}{b} \equiv 1, \quad c^2(t) = \frac{1}{16}\sin^2(2t).$$

One can see that the data for τ large fit with the data of $\mathbb{P}(1, 1, 4)$ very well. Again, we know that τ going to $+\infty$ is equivalent to β going to $1/4$. So the numerical result implies the expected result: as $\beta \to 1/4$, the metric ω_β converges to the orbifold Kähler–Einstein metric $\hat{\omega}_{KE}$ on $P(1, 1, 4)$.

5.2 $\mathbb{Z}_2$-Quotient of Eguchi–Hanson as the Bubble

As pointed out by Dr. H-J. Hein and Professor LeBrun, if we rescale the metric near the orbit $\mathrm{Orb}_{R=0} = \mathbb{RP}^2$ appropriately, then the rescaled metrics should converge to another well-known metric, which is the $\mathbb{Z}_2$ quotient of the Eguchi–Hanson metric. This kind of metric was studied in much generality by Stenzel [5]. It is easy to see this convergence from the discussion in Sect. 3 and the following numerical results. For this we use the explicit description of this metric in [5, Section 7], which says that, away from $\mathbb{RP}^2$ the $\mathbb{Z}_2$-quotient of the Eguchi–Hanson metric can be pulled back to an $SO(3)$ invariant metric on $(0, \infty) \times SO(3)$ with the following expression:

$$g = \cosh s(ds)^2 + \sinh s \tanh s(X_1^*)^2 + \cosh s((X_2^*)^2 + (X_3^*)^2). \tag{12}$$

As before, we can let $a^*(s) = \sqrt{\sinh s \tanh s}$, $b^*(s) = c^*(s) = \sqrt{\cosh s}$. Let t^* be the distance function to the orbit $\mathbb{RP}^2$. Then from (12), we see the following relation:

$$\frac{ds}{dt^*} = \frac{1}{\sqrt{\cosh s}} = \frac{1}{c^*(s)}, \quad \frac{a^*}{b^*}(s) = \tanh s.$$

If we compare these identities with (8) and (9), we see that the coordinate r is preserved under this convergence. In other words, $r = -s$ and $\frac{a^*}{b^*} = \frac{a}{b} = -\tanh r$. To prove the convergence, we only need to prove the convergence of rescaled data as functions of r.

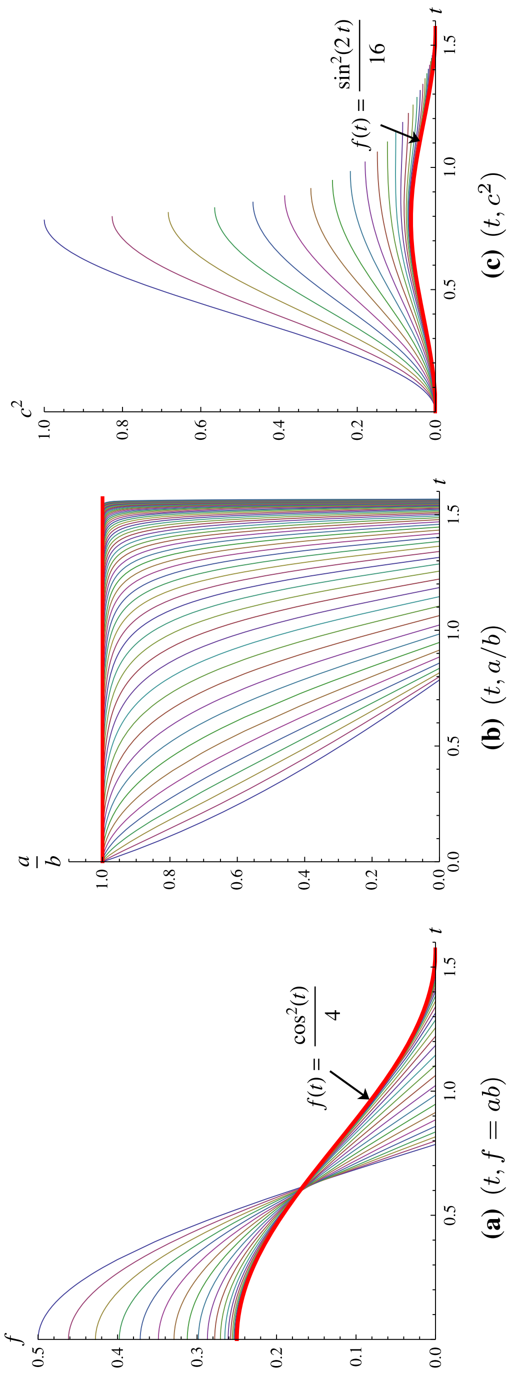

Fig. 5 Convergence of data

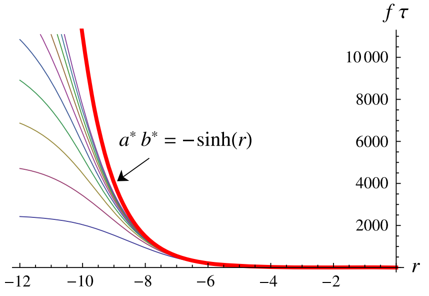

(a) $(r, \tau f)$

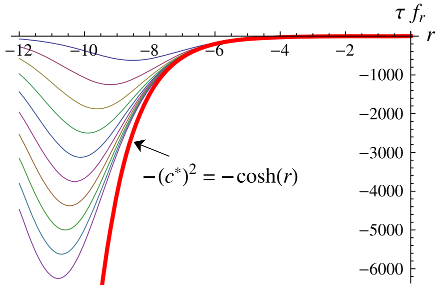

(b) $(r, \tau f_r)$

Fig. 6 Bubbling

Note that, since the length scale of $\mathrm{Orb}_{R=0} = \mathbb{RP}^2$ is $1/\sqrt{\tau}$ as $\tau \to +\infty$ (equivalently as $\beta \to 1/4$), we need to use the scale factor τ to rescale the metric back. So we need to show the following convergence.

$$\lim_{\tau\to+\infty} f\tau = \lim_{\tau\to+\infty} a(r,\tau)b(r,\tau)\cdot\tau = a^*b^* = -\sinh r,$$
$$\lim_{\tau\to+\infty} f_r\tau = \lim_{\tau\to+\infty} -c(r,\tau)^2\tau = -(c^*)^2 = -\cosh r.$$

Figure 6 shows the convergence of numerical data for $\tau = 10,000 * i$, $i = 1, \ldots, 10$.

6 Data of $\mathbb{P}^1 \times \mathbb{P}^1$ and Associated Sasaki–Einstein Metric

We have the following Segre embedding of $\mathbb{P}^1 \times \mathbb{P}^1$ into $\mathbb{P}^3$ by the complete linear system $|H_1 + H_2|$, where H_1 and H_2 are the hyperplane divisors of the two factors of $\mathbb{P}^1$, respectively.

$$\begin{aligned} \phi : \mathbb{P}^1 \times \mathbb{P}^1 &\longrightarrow \mathbb{P}^3 \\ ([U_0, U_1], [V_0, V_1]) &\mapsto [U_0V_0 + U_1V_1, \\ &\quad \sqrt{-1}(U_0V_0 - U_1V_1), U_0V_1 + U_1V_0, U_0V_1 - U_1V_0]. \end{aligned} \tag{13}$$

Note that

$$\phi(\mathbb{P}^1 \times \mathbb{P}^1) = \{[Z_1, Z_2, Z_3, Z_4] \in \mathbb{P}^3; Z_1^2 + Z_2^2 + Z_3^2 = Z_4^2\}.$$

Lemma 6.1 *Let $p_i : \mathbb{P}^1 \times \mathbb{P}^1 \to \mathbb{P}^1$ be the projection to the i-th $\mathbb{P}^1$-factor and $\omega_{\mathbb{P}^N}$ denote the standard Fubini–Study metric on $\mathbb{P}^N$ in the cohomology class $2\pi c_1(\mathcal{O}_{\mathbb{P}^N}(1))$. Then the Segre embedding ϕ satisfies*

$$\phi^*\omega_{\mathbb{P}^2} = p_1^*\omega_{\mathbb{P}^1} + p_2^*\omega_{\mathbb{P}^1}.$$

Proof This follows from the following formula:

$$\begin{aligned} p_1^*\omega_{\mathbb{P}^1} + p_2^*\omega_{\mathbb{P}^1} &= \sqrt{-1}\partial\bar{\partial}\log((|U_0|^2+|U_1|^2)(|V_0|^2+|V_1|^2)) \\ &= \sqrt{-1}\partial\bar{\partial}\log\Big(|U_0V_0+U_1V_1|^2+|\sqrt{-1}(U_0V_0-U_1V_1)|^2 \\ &\quad +|U_0V_1+U_1V_0|^2+|U_0V_1-U_1V_0|^2\Big). \end{aligned}$$

□

Now $SO(3)$ acts on $\mathbb{C}^4$ by

$$g\cdot(Z_1,Z_2,Z_3,Z_4)=(g\cdot(Z_1,Z_2,Z_3),Z_4).$$

This induces an action of $SO(3)$ on $\phi(\mathbb{P}^1\times\mathbb{P}^1)$.

We will calculate the data associated with the product metric $\tilde{\omega} := p_1^*\omega_{\mathbb{P}^1} + p_2^*\omega_{\mathbb{P}^1}$ using a method similar to the one in Sect. 2. We use the following notation:

$$(Z_1,Z_2,Z_3,Z_4)\sim e^{-i\operatorname{Arg}(Z_1^2+Z_2^2+Z_3^2)/2}(Z_1,Z_2,Z_3,Z_4)=:(u+iv,z_4).$$

Here $u, v\in\mathbb{R}^3$, $z_4\in\mathbb{C}$. In this notation, we have

$$\phi(\mathbb{P}^1\times\mathbb{P}^1)=\{(u+iv,z_4);|u|^2-|v|^2=z_4^2, 0\neq(u+iv,z_4)\in\mathbb{C}^3\times\mathbb{R}\}/\sim.$$

We can calculate the infinitesimal vector field of basis of $so(3)$, at point $(u+iv,\sqrt{|u|^2-|v|^2})$:

$$T_u=(-\sqrt{-1}|v|e_w,0),\quad T_v=(|u|e_w,0),\quad T_w=(-|u|e_v+\sqrt{-1}|v|e_u,0).$$

As in Sect. 3.1, we define $R=\frac{|v|}{|u|}$ and calculate the radial vector field as

$$T_R=\left(\sqrt{-1}|u|e_v,-\frac{|u|R}{\sqrt{1-R^2}}\right).$$

Here for clarity, we will use $\overline{T}_u,\overline{T}_v,\overline{T}_w$, and $\overline{T}_R$ to denote the tangent vector in $T_{[u+iv]}\mathbb{P}^2$ determined by T_u,T_v,T_w,T_R, respectively. The lengths of these tangent vectors in $T_{[u+iv,iz_3]}\phi(\mathbb{P}^1\times\mathbb{P}^1)$ can be calculated as in Example 3.1:

$$|\overline{T}_u|^2_{\tilde{\omega}}=\frac{R^2}{2},\quad |\overline{T}_v|^2_{\tilde{\omega}}=\frac{1}{2},\quad |\overline{T}_w|^2_{\tilde{\omega}}=\frac{1-R^2}{2},\quad |\overline{T}_R|^2_{\tilde{\omega}}=\frac{1}{2(1-R^2)}.$$

By transforming the variable R into the distance variable $\tilde{t}$ under the metric $\tilde{\omega}$, we get:

$$\frac{d\tilde{t}}{dR}=\frac{1}{2(1-R^2)}\ \textit{and}\ \tilde{t}(1)=0\Longrightarrow R(\tilde{t})=\cos(\sqrt{2}\tilde{t}),\ 0\le\tilde{t}\le\frac{\pi}{2\sqrt{2}}, \tag{14}$$
$$|\overline{T}_u|_{\tilde{\omega}}=\frac{1}{\sqrt{2}}\cos(\sqrt{2}\tilde{t}),\quad |\overline{T}_v|_{\tilde{\omega}}=\frac{1}{\sqrt{2}},\quad |\overline{T}_w|_{\tilde{\omega}}=\frac{1}{\sqrt{2}}\sin(\sqrt{2}\tilde{t}).$$

Note that $\tilde{\omega} = p_1^*\omega_{\mathbb{P}^1} + p_2^*\omega_{\mathbb{P}^1}$ has Ricci curvature equal to 2. To normalize the Ricci curvature to be 3, we just need to rescale the metric. So by letting $\omega = \frac{2}{3}\omega_{\mathbb{P}^1\times\mathbb{P}^1}$ and redefining $t = \sqrt{2}\tilde{t}/\sqrt{3}$ we get the following result, which are the same data as in Example 3.2.

$$a = \frac{1}{\sqrt{3}}\cos(\sqrt{3}t), \quad b = \frac{1}{\sqrt{3}}, \quad c = \frac{1}{\sqrt{3}}\sin(\sqrt{3}t); \quad 0 \le t \le \frac{\pi}{2\sqrt{3}}. \tag{15}$$

Let $\mathrm{Aff}(\mathbb{P}^1 \times \mathbb{P}^1)$ be the affine cone over $\phi(\mathbb{P}^1 \times \mathbb{P}^1) \subset \mathbb{P}^3$:

$$\mathrm{Aff}(\mathbb{P}^1 \times \mathbb{P}^1) = \{(Z_1, Z_2, Z_3, Z_4) \in \mathbb{C}^4; Z_1^2 + Z_2^2 + Z_3^2 = Z_4^2\}.$$

In the following, we use L to denote the total space of the line bundle $p_1^*\mathcal{O}(-H_1) + p_2^*\mathcal{O}(-H_2)$. Then $L = Bl_0\mathrm{Aff}(\mathbb{P}^1 \times \mathbb{P}^1)$. In other words, the zero section S_0 of L can be blown down to get a singular variety L/S_0 which is isomorphic to the affine cone $\mathrm{Aff}(\mathbb{P}^1 \times \mathbb{P}^1)$. Moreover, the line bundle L has a Hermitian metric $h := h_{\mathbb{P}^1\times\mathbb{P}^1}$ whose Chern curvature is $-\tilde{\omega} = -(p_1^*\omega_{\mathbb{P}^1} + p_2^*\omega_{\mathbb{P}^1})$, i.e., we have the identity:

$$-\sqrt{-1}\partial\bar{\partial}\log h = -\tilde{\omega} = -(p_1^*\omega_{\mathbb{P}^1} + p_2^*\omega_{\mathbb{P}^1}). \tag{16}$$

Now $h : L \ni s \to |s|_h^2$ is a smooth function on L which induces a smooth function h on $L/S_0 \cong \mathrm{Aff}(\mathbb{P}^1 \times \mathbb{P}^1)$. Up to a scaling factor, we see that

$$\begin{aligned} h : \mathrm{Aff}(\mathbb{P}^1 \times \mathbb{P}^1) &\to \mathbb{R}^{\ge 0} \\ (Z_1, Z_2, Z_3, Z_4) &\mapsto |Z|^2 = |Z_1|^2 + |Z_2|^2 + |Z_3|^2 + |Z_4|^2. \end{aligned}$$

Define $M^5 \subset L$ to be the unit circle bundle, i.e., $M^5 = \{s \in L; |s|_h^2 = 1\}$. Then

$$M^5 \cong \{(Z_1, Z_2, Z_3, Z_4); Z_1^2 + Z_2^2 + Z_3^2 = Z_4^2, |Z|^2 = 1\} = \mathrm{Aff}(\mathbb{P}^1 \times \mathbb{P}^1) \cap S^7.$$

We know that there exists a Sasaki–Einstein metric on M^5. Now we will calculate this Sasaki–Einstein metric on M^5 by calculating the data in the sense of [3]. To do this we will first calculate the metric on M^5 induced by the standard Euclidean metric on $\mathbb{C}^4$. Then we modify the metric appropriately (rescale it in different directions) to get the desired Sasaki–Einstein metric.

Lemma 6.2 *On $M^5 = S^7 \cap \mathrm{Aff}(\mathbb{P}^1 \times \mathbb{P}^1)$, we have*

$$|u| = \frac{1}{\sqrt{2}}, \quad |v| = \frac{\cos(\sqrt{2}\tilde{t})}{\sqrt{2}}. \tag{17}$$

Proof On M^5, we have the identities $|u|^2 - |v|^2 = z_4^2$ and $|u|^2 + |v|^2 + |z_4|^2 = 1$. So we get $|u| = 1/\sqrt{2}$. The second identity follows from (14) and $|v| = R|u|$. □

Now $G = SO(3) \times U(1)$ acts on $\mathbb{C}^4$ by

$$(g, e^{i\theta}) \cdot (Z_1, Z_2, Z_3, Z_4) = \left(e^{i\theta} g(Z_1, Z_2, Z_3), e^{i\theta} Z_4\right).$$

The generic orbit is of codimension 1. $\mathrm{Aff}(\mathbb{P}^1 \times \mathbb{P}^1)$ is G-invariant under this action. Fix the standard basis of $so(3) \oplus u(1)$ by adjoining the generator X_4 of $u(1)$ to the standard basis of $so(3)$ used above. We will denote the infinitesimal vector fields by the same notation. So we have

$$X_1 = T_u, X_2 = T_v, X_3 = T_w, X_4 = (-v + iu, iz_4).$$

Proposition 6.1 *Considering M^5 as a submanifold in $(\mathbb{C}^4, g_{\text{flat}})$, $T_{(u+iv,z_4)}\mathbb{C}^4 = \mathbb{R}^8$ has an orthonormal basis given by*

$$\begin{aligned}
\partial_{\tilde{r}} &= (u + iv, z_4),\\
\tilde{\mathfrak{e}}_0 &= \partial_\theta = X_4 = (-v + iu, iz_4),\\
\tilde{\mathfrak{e}}_1 &= \partial_{\tilde{t}} = -\sqrt{2}\sin(\sqrt{2}\tilde{t})T_R = (-\sqrt{-1}\sin(\sqrt{2}\tilde{t})e_v, \cos(\sqrt{2}\tilde{t})),\\
\tilde{\mathfrak{e}}_2 &= \frac{\sqrt{2}}{\sin(\sqrt{2}\tilde{t})}(-X_3 + \cos(\sqrt{2}\tilde{t})X_4) = (\sin(\sqrt{2}\tilde{t})e_v, \sqrt{-1}\cos(\sqrt{2}\tilde{t})),\\
\tilde{\mathfrak{e}}_3 &= \frac{\sqrt{2}}{\cos(\sqrt{2}\tilde{t})}X_1 = (-\sqrt{-1}e_w, 0),\\
\tilde{\mathfrak{e}}_4 &= \sqrt{2}X_2 = (e_w, 0).
\end{aligned}$$

We have the relation

$$J\partial_{\tilde{r}} = i\partial_{\tilde{r}} = \partial_\theta, \quad J\tilde{\mathfrak{e}}_1 = i\tilde{\mathfrak{e}}_1 = \tilde{\mathfrak{e}}_2, \quad J\tilde{\mathfrak{e}}_3 = i\tilde{\mathfrak{e}}_3 = \tilde{\mathfrak{e}}_4.$$

Under the induced metric on M^5 by the standard Euclidean metric on $\mathbb{C}^4$, $T_{(u+iv,z_4)}M^5$ has an orthonormal basis $\{\partial_\theta, \tilde{\mathfrak{e}}_1, \tilde{\mathfrak{e}}_2, \tilde{\mathfrak{e}}_3, \tilde{\mathfrak{e}}_4\}$. Moreover, let $S^1 \to M^5 \to \mathbb{P}^1 \times \mathbb{P}^1$ be the fibration structure. Then the vertical unit vector field is generated by ∂_θ, and the space of horizontal vector fields in the tangent space has an orthonormal basis consisting of $\{\tilde{\mathfrak{e}}_1, \tilde{\mathfrak{e}}_2, \tilde{\mathfrak{e}}_3, \tilde{\mathfrak{e}}_4\}$.

Proof First it is easy to see that $J\partial_{\tilde{r}} = \partial_\theta$ and $\partial_{\tilde{r}} \perp Span(\{\partial_\theta, X_i, i = 1, 2, 3, 4\})$. We can also verify that $Span\{X_1, X_2\} \perp Span(\{\partial_\theta, X_3, X_4\})$ and $T_R \perp Span(\{\partial_\theta, X_i, i = 1, 2, 3, 4\})$. The lemma follows by orthonormalization. □

Lemma 6.3 *Considering h as a smooth function on L as above, the Sasaki–Einstein metric on M^5 is given by*

$$g_{SE} = \frac{1}{2}\left(\sqrt{-1}\partial\bar{\partial}h^{2/3}\right)(\cdot, J\cdot)|_{M^5}.$$

Proof If M^5 is a Sasaki–Einstein metric, then the metric cone $C(M^5)$ is a Ricci-flat Kähler metric. In our case, $C(M^5) \cong L/S_0$ as the affine variety with an isolated singular point. So we only need to construct the rotationally symmetric Ricci-flat Kähler metric on $C(M^5) \cong L/S_0$ and restrict to $M^5 \cong \{h = 1\} \cap C(M^5)$ to get the Sasaki–Einstein metric on M^5.

In general, assume $L \to D_0$ is a line bundle with a Hermitian metric h such that $\sqrt{-1}\partial\bar{\partial}\log h = \tilde{\omega}$ is a Kähler–Einstein metric, satisfying $Ric(\tilde{\omega}) = \tau\tilde{\omega}$. Then we can define the rotationally symmetric Kähler metric on the total space on L/S_0 using the potential h^δ, i.e., we define

$$\Omega_\delta = \sqrt{-1}\partial\bar{\partial}h^\delta = \delta h^\delta\tilde{\omega} + \delta^2 h^\delta \frac{\nabla\xi \wedge \overline{\nabla\xi}}{|\xi|^2}. \tag{18}$$

The Ricci curvature of Ω_δ on $L\backslash D_0$ is given by

$$\begin{aligned} Ric(\Omega_\delta) &= -\sqrt{-1}\partial\bar{\partial}\log\Omega_\delta^n = -(d+1)\sqrt{-1}\partial\bar{\partial}\log h^\delta + Ric(\tilde{\omega}) \\ &= \pi^*(-(d+1)\delta\tilde{\omega} + \tau\tilde{\omega}). \end{aligned}$$

This is zero if and only if $\delta = \tau/(d+1)$. In our case, $\tau = 2, d = 2$. So $\delta = 2/3$. □

Theorem 6.1 *The Sasaki–Einstein metric on M^5 has an orthonormal basis given by*

$$\begin{aligned} \mathfrak{e}_0 &= \frac{3}{2}X_4, \\ \mathfrak{e}_1 &= \partial_t = -\sqrt{3}\sin(\sqrt{3}t)T_R, \\ \mathfrak{e}_2 &= \frac{\sqrt{3}}{\sin(\sqrt{3}t)}(-X_3 + \cos(\sqrt{3}t)X_4), \\ \mathfrak{e}_3 &= \frac{\sqrt{3}}{\cos(\sqrt{3}t)}X_1, \\ \mathfrak{e}_4 &= \sqrt{3}X_2. \end{aligned}$$

Proof First note that the induced metric on M^5 by flat metric is given by $\frac{1}{2}\sqrt{-1}\partial\bar{\partial}h$. By the formula (18), we see that if we change the potential from h to h^δ, then the vertical metric scales by δ^2, and the horizontal part of the metric scales by δ. Since $\delta = 2/3$ now, the theorem follows from Proposition 6.1. □

Corollary 6.1 *1. Under the Sasaki–Einstein metric on M^5, there is an orthonormal basis of T^*M^5 given by*

$$\begin{aligned} &\alpha := \frac{2}{3}(X_4^* + \cos(\sqrt{3}t)X_3^*), \\ &\mathfrak{e}^1 = dt, \quad \mathfrak{e}^2 = -\frac{\sin(\sqrt{3}t)}{\sqrt{3}}X_3^*, \\ &\mathfrak{e}^3 = \frac{\cos(\sqrt{3}t)}{\sqrt{3}}X_1^*, \quad \mathfrak{e}^4 = \frac{1}{\sqrt{3}}X_2^*. \end{aligned}$$

2. *If we define* $\omega_1 = e^1\wedge e^2+e^3\wedge e^4$, $\omega_2 = e^1\wedge e^3+e^4\wedge e^2$ *and* $\omega_3 = e^1\wedge e^4+e^2\wedge e^3$, *the following identities hold:*

$$d\alpha = 2\omega_1, \quad d\omega_2 = -3\alpha\wedge\omega_3 + 2X_4^*\wedge\omega_3, \quad d\omega_3 = 3\alpha\wedge\omega_2 - 2X_4^*\wedge\omega_2.$$

This gives the $SU(2)$ *structure in the sense of [3].*

Remark 6.1 Item 2 in Corollary 6.1 follows from item 1 and the fomula $dX_i^* = -\epsilon_{ijk}X_j^*\wedge X_k^*$. As explained in [3], because we are using the G-invariant forms on $G\times(t_-,t_+)$ to represent the data, there is an extra term $2X_4^*\wedge\omega_3$. The coefficient 2 comes from the fact that $(e^{i\theta})^*\mathcal{S} = e^{2i\theta}\cdot\mathcal{S}$, where we use $\mathcal{S}$ to denote the nowhere vanishing holomorphic volume form on $\mathcal{M} = \mathrm{Aff}(\mathbb{P}^1\times\mathbb{P}^1)$, which can be given by the Poincaré residue formula:

$$\mathcal{S} = Res_{\mathcal{M}}(dZ_1\wedge dZ_2\wedge dZ_3\wedge dZ_4) = -\frac{dZ_1\wedge dZ_2\wedge dZ_3}{Z_4}.$$

Remark 6.2 By a similar calculation, we can calculate the data associated on the standard round S^5 under the $SO(3)$ action:

$$g\cdot(Z_1,Z_2,Z_3) = (g(Z_1,Z_2,Z_3)).$$

The result is as follows. For the orthonormal basis of TS^5, we have

$$\begin{aligned}
&\mathfrak{e}_0 = \partial_\theta = X_4,\\
&\mathfrak{e}_1 = \partial_t, \quad \mathfrak{e}_2 = \frac{1}{\sin(2t)}(-X_3+\cos(2t)X_4),\\
&\mathfrak{e}_3 = \frac{X_1}{\sin\left(\frac{\pi}{4}-t\right)}, \quad \mathfrak{e}_4 = \frac{X_2}{\cos\left(\frac{\pi}{4}-t\right)}.
\end{aligned}$$

So the corresponding orthonormal basis of T^*S^5 is

$$\begin{aligned}
&\alpha := \mathfrak{e}^0 = X_4^* + \cos(2t)X_3^*,\\
&\mathfrak{e}^1 = dt, \quad \mathfrak{e}^2 = -\sin(2t)X_3^*,\\
&\mathfrak{e}^3 = \sin\left(\frac{\pi}{4}-t\right)X_1^*, \quad \mathfrak{e}^4 = \cos\left(\frac{\pi}{4}-t\right)X_2^*.
\end{aligned}$$

The corresponding $SU(2)$-structural equations are

$$d\alpha = 2\omega_1, \quad d\omega_2 = -3\alpha\wedge\omega_3 + 3X_4^*\wedge\omega_3, \quad d\omega_3 = 3\alpha\wedge\omega_2 - 3X_4^*\wedge\omega_2.$$

Remark 6.3 There is a statement in Theorem 1 in [3]: "There is no solution of (23) that defines an Einstein-Sasaki metric on a compact manifold". The above two special examples show that this statement is not correct. By going through the proof, we find that some error happens in Lemma 4, where, in the second case, the assumption $q\neq 0$ is made. In our notation, this assumption implies the isotopy group of special orbit has a generator whose X_4-component is nonzero. But this is not true in the above examples. Actually, it is easy to verify that

1. For $t = 0$, $H_- \cong U(1)$ with Lie algebra $\mathfrak{h} = \langle -X_3 + X_4 \rangle$.
2. For $t = \frac{\pi}{2\sqrt{3}}$, $H_+ \cong U(1) = U(1)_1$ with Lie algebra $\mathfrak{h} = \langle X_1 \rangle$.

Because the action $U(1)_1$ has generator X_1, which has no contribution from X_4, so $q = 0$ for H_+. It would be interesting to classify the missing cohomogeneity one Sasaki–Einstein 5-manifolds for which $q = 0$.

Acknowledgments The author would like to thank Dr. S. Sun and Dr. H-J. Hein for insightful suggestions, and Professor LeBrun for his interest in our work. The author would also like to thank Dr. C. Koca for carefully reading the previous version of the paper and pointing out several typos.

Appendix

The following is the Mathematica code that generates the figures that appear above.

1. Figure 1
   ```
   S=Table[ NDSolve[ {f'[t] == h[t], h'[t] == 12 f[t]*h[t] + 2 Coth[2 t]*h[t] − h[t]^2/f[t], f[−10^(−5)] == 10^(−5), h[−10^(−5)] == −1}, {f, h}, {t, −100, −10^(−5)}],{i,3,15}];
   Plot[Evaluate[h[t] /. S], {t, −18, −10^(−5)}, AxesLabel -> {r, f}]
   Plot[Evaluate[h[t] /. S], {t, −18, −10^(−5)}, AxesLabel -> {r, Subscript[f, r]}, PlotRange -> {{−18, 0}, {−0.13, 0}}, AxesLabel-> {r, Subscript[f,r]}]
   ```

2. (a) Figure 2(a)
   ```
   S2=Table[ NDSolve[{f'[t] == h[t], h'[t] == 12 f[t]*h[t] + 2 Coth[2 t]*h[t] − h[t]^2/f[t], f[−10^(−5)] == 10^(−5)/(0.5+0.1*i), h[−10^(−5)] == −1/(0.5 +0.1*i)}, {f, h}, {t, −500, −10^(−5)}],{i,0,300}];
   A2=Evaluate[f[−500]/.S2];
   ListLinePlot[{Join[Table[{0.5+0.1*i},{i,0,300}],A2,2],{{0,0.25},{30,0.25}}, {{1,0},{1,0.5},{0,0.5}},{{3,0},{3,1/3},{0,1/3}},{{6.73,0},{6.73,5/18}, {0,5/18}}},
   PlotRange->{{0,22},{0.2,0.8}}, AxesLabel->{τ, α^2}]
   ```
   (b) Figure 2(b)
   ```
   S3=Table[ NDSolve[{f'[t] == h[t], h'[t] == 12 f[t]*h[t] + 2 Coth[2 t]*h[t] − h[t]^2/f[t], f[−10^(−5)] == 10^(−5)/(100*i), h[−10^(−5)] == −1/(100*i)}, {f, h}, {t, −500, −10^(−5)}],{i,1,50}];
   A3=Evaluate[f[−500]/.S3];
   ListLinePlot[{Join[Table[{100*i},{i,1,50}],A3,2],{{500,0.25},{5000,0.25}},
   PlotRange->{{500,5000},{0.249998,0.250008}}, AxesLabel->{τ, α^2}]
   ```

3. Figure 3
   ```
   s1= NDSolve[{f1'[t] == h1[t], h1'[t] == 12 f1[t]*h1[t] + 2 Coth[2 t]*h1[t] − h1[t]^2/f1[t], f1[−10^(−5)] == 10^(−5), h1[−10^(−5)] == −1, {f1, h1}, {t, −100, −10^(−5)}];
   ```

s2= NDSolve[{f2'[t] == h2[t], h2'[t] == 12 f2[t]*h2[t] + 2 Coth[2 t]*h2[t] − h2[t]^2/f2[t], f2[−10^(−5)] == 10^(−5)/3, h2[−10^(−5)] == −1/3}, {f2, h2}, {t, −100, −10^(−5)}];
s3= NDSolve[{f3'[t] == h3[t], h3'[t] == 12 f3[t]*h3[t] + 2 Coth[2 t]*h3[t] − h3[t]^2/f3[t], f3[−10^(−5)] == 10^(−5)/6.73, h3[−10^(−5)] == −1/6.73}, {f3, h3}, {t, −100, −10^(−5)}];
Plot[{Evaluate[f1[t] /. s1],Evaluate[f2[t] /. s2],Evaluate[f3[t] /. s3]}, {t, −10, −10^(−5)},
PlotRange -> {{−10, −10^(−5)}, {−0.1, 0.6}}, AxesLabel ->{r,f}]
Plot[{Evaluate[h1[t] /. s1],Evaluate[h2[t] /. s2],Evaluate[h3[t] /. s3]}, {t, −8, −10^(−5)},
PlotRange -> {{−5, 0}, {−1.1, 0.1}}, AxesLabel -> {r, f_r}]

4. Figure 4
   (a) Figure 4(a)
   V=Table[NDSolve[{f'[t] == h[t], h'[t] == 12 f[t]*h[t] + 2 Coth[2 t]*h[t] − h[t]^2/f[t], f[−10^(−5)] == 10^(−5)/(100*i), h[−10^(−5)] == −1/(100*i)}, {f, h}, {t, −500, −10^(−5)}],{i,1,50}];
   Clen=Re[Sqrt[-Evaluate[h[t]/.V]]]; Diam=NIntegrate[Clen,t,−200,−0.001];
   ListLinePlot[{ Table[{0.2*i, Extract[Flatten[Diam],i]},{i,1,50}], {{1,0}, {1, Pi/4}, {0, Pi/4}}, {{3,0}, {3, Pi/(2Sqrt[3])},{0, Pi/(2Sqrt[3])}}, {{6.73,0}, {6.73, 1.064}, {0, 1.064}}, Table[{i, Pi/2}, {i, 0, 10}]}, PlotRange -> {{0, 10}, {0.5, 1.6}}, AxesLabel->{τ, $t_{\max}$}]
   (b) Figure 4(b)
   LV=Table[NDSolve[{f'[t] == h[t], h'[t] == 12 f[t]*h[t] + 2 Coth[2 t]*h[t] − h[t]^2/f[t], f[−10^(−5)]==10^(−5)/(4,00*i), h[−10^(−5)]==−1/(4,000*i)}, {f, h}, {t, −500, −10^(−5)}],{i,1,50}];
   LC=Re[Sqrt[-Evaluate[h[t]/.LV]]]; LD=NIntegrate[LC,t,−500,−0.001];
   ListLinePlot[{ Table[{4000*i, Extract[Flatten[LD],i]},{i,1,50}], Table[{4,000*i, Pi/2}, {i, 1, 50}]}, PlotRange -> {{4,000, 200,000}, {1.45, 1.65}}, AxesLabel->{τ, $t_{\max}$}]

5. Figure 5
   K = 60; CV = Table[NDSolve[{f'[t] == h[t], h'[t] == 12 f[t]*h[t] + 2 Coth[2 t]*h[t] − h[t]^2/f[t], f[−10^(−5)] == 10^(−5)/(1.1^(2 i)), h[−10^(−5)] == −1/(1.1^(2 i))}, {f, h}, {t, −100, −0.001}], {i, 0, K}]; CC = Re[Sqrt[-Evaluate[h[t] /. CV]]];
   CT = Table[NDSolve[{g'[t] == Extract[Flatten@CC, i], g[−100] == 0}, g, {t, −100, −0.001}], {i, 1, K}];
   T1 = Table[Flatten@Evaluate[{g[t] /. Part[CT, i], f[t] /. Part[CV, i]}], {i, 1, K}];
   T2 = Table[Flatten@Evaluate[{g[t] /. Part[CT, i], -h[t] /. Part[CV, i]}], {i, 1, K}];
   T3 = Table[{Evaluate[g[t] /. Part[CT, i]], -Tanh[t]}, {i, 1, K}];
   PF = ParametricPlot[T1, {t, −100, −0.001}, PlotStyle -> Thickness[0.002], PlotRange -> {{0, 1.6}, {0, 0.5}}, AspectRatio -> 1, AxesLabel -> {t, f}];
   PH = ParametricPlot[T2, {t, −100, −0.001}, PlotStyle -> Thickness[0.002], PlotRange -> {{0, 1.6}, {0, 1}}, AspectRatio -> 1, AxesLabel -> {t, c^2}];
   PR = ParametricPlot[T3, {t, −100, −0.001}, PlotStyle -> Thickness[0.002], PlotRange ->{{0, 1.6}, {0, 1.1}}, AspectRatio -> 1, AxesLabel -> {t, a/b}];

PA = ParametricPlot[{t, Cos[t]^2/4}, {t, 0, Pi/2}, PlotStyle -> {Red, Thickness[0.01]}];
PB = ParametricPlot[{t, Sin[2 t]^2/16},{t, 0, Pi/2}, PlotStyle -> {Red, Thickness[0.01]}];
PC = Plot[1, {t, 0, Pi/2}, PlotStyle -> {Red, Thickness[0.01]}];
Show[PF, PA] Show[PH, PB] Show[PR, PC]

6. Figure 6
Bu = Table[NDSolve[{f'[t] == h[t], h'[t] == 12 f[t]*h[t] + 2 Coth[2 t]*h[t] − h[t]^2/f[t], f[−10^(−5)] == 10^(−5)/(10,000*i), h[−10^(−5)] == −1/(10,000*i)}, {f, h}, {t, −100, −0.001}], {i, 1, 10}];
Bu1 = Table[10,000*i, {i, 1, 10}]*Flatten@Evaluate[f[t] /. Bu];
Bu2 = Table[10,000*i, {i, 1, 10}]*Flatten@Evaluate[h[t] /. Bu];
BP1 = Plot[Bu1, {t, −12, 0}, AxesLabel -> {r, τ}];
BP2 = Plot[Bu2, {t, −12, 0}, AxesLabel -> {r, τ}];
EH1 = Plot[−Sinh[t], {t, −12, 0}, PlotStyle -> {Thickness[0.01], Red}];
EH2 = Plot[−Cosh[t], {t, −12, 0}, PlotStyle -> {Thickness[0.01], Red}];
Show[BP1, EH1] Show[BP2, EH2]

References

1. Li, C., Sun, S.: Conical Kähler-Einstein metrics revisited. arXiv:1207.5011
2. Gauntlett, J., Martelli, D., Sparks, J., Yau, S.-T.: Obstructions to the existence of Sasaki–Einstein metrics. Commun. Math. Phys. **273**(3), 803–827 (2007)
3. Conti, D.: Cohomogeneity one Einstein–Sasaki 5-manifolds. Commun. Math. Phys. **274**(3), 751–774 (2007)
4. Dancer, A.S., Strachan, Ian A.B.: Kähler–Einstein metrics with $SU(2)$ action. Math. Proc. Camb. Philos. Soc. **115**, 513 (1994)
5. Stenzel, M.B.: Ricci-flat metrics on the complexification of a compact rank one symmetric space. Manuscr. Math. **80**(1), 151–163 (1993)